Modeling of the Singlet Oxygen Distribution in Photofrin-Photodynamic Therapy of the Plural Cavity

Rozhin Penjweini [1], Michele M. Kim [1, 2], and Timothy C. Zhu [1]

[1] Department of Radiation Oncology, School of Medicine, University of Pennsylvania, Philadelphia, PA 19104, USA, [2] Department of Physics and Astronomy, University of Pennsylvania, Philadelphia, PA 19104, USA

*Corresponding author: tzhu@mail.med.upenn.edu, phone 215-662-4043

Abstract: Photofrin-mediated photodynamic therapy (PDT) is used after surgical resection at the University of Pennsylvania to treat the microscopic disease for malignant pleural mesothelioma and to increase survival rate. When Photofrin is exposed to laser light at 630 nm in well-oxygenated tissue, it produces reacted singlet oxygen ($[^1O_2]_{rx}$) that kills cancer cells. As $[^1O_2]_{rx}$ is imperative to PDT treatment efficacy, in this study we use COMSOL Multiphysics software to simulate the distribution of $[^1O_2]_{rx}$ on every point of the plural cavity surface that is being treated. The geometry of the pleural cavity that is used in this study was obtained during the surgery using an infrared camera–based navigation system (NDI). The initial Photofrin concentration inside the pleural cavity and the light fluence information used for the simulation of $[^1O_2]_{rx}$ were measured during the treatment.

Keywords: PDT, Photofrin, tissue oxygenation, reacted singlet oxygen concentration, light fluence distribution.

1. Introduction

Type II photodynamic therapy (PDT) is based on the photochemical reaction among a photosensitizing agent (photosensitizer), light at a specific wavelength, and tissue oxygen concentration ($[^3O_2]$), which generates reacted singlet oxygen ($[^1O_2]_{rx}$) to cause cell death (1,2). In the treatment of malignant pleural mesothelioma at the Hospital of the University of Pennsylvania, Photofrin-mediated PDT is coupled with surgical resection of the tumor as local treatment. As accurate light dosimetry is imperative to PDT effect, an infrared camera–based navigation system (NDI) is used to display the cumulative light fluence on every point of the plural cavity surface that is being treated (3,4). The concentration of Photofrin photosensitizer inside the pleural cavity is also measured using a multi-fiber contact spectroscopy probe (5). Although extensive work has been done to monitor the light and photosensitizer distribution on the surface of the plural cavity (4,6,7), the spatial distribution of $[^1O_2]_{rx}$ has not been investigated.

As the primary mediator of cell damage during type II PDT, $^1O_2$ is a good dosimetric quantity to evaluate the treatment outcome. Therefore, in this study, the distribution of $[^1O_2]_{rx}$ on the surface of the plural cavity is simulated by using the information that was obtained during the treatment regarding the geometry of the plural cavity, concentration of Photofrin, and the distribution of light fluence.

2. Obtaining Geometry of Pleural Cavity and Delivered Light Fluence

The treatment delivery wand is comprised of a modified endotrachial tube filled with scattering media and an optical fiber inside the tube to deliver the light. The position of the treatment is tracked using an attachment that has nine reflective passive markers that are seen by an IR camera. The collected position points were processed and plotted as a three dimensional volume of the pleural cavity using Matlab and MeshLab software as published previously (8,9). Light delivery information was calculated for the PDT treatment using information regarding the geometry of the cavity and the position of the treatment delivery system. The cumulative light fluence on every point of the cavity surface that is being treated was found (3,4).

3. PDT Photochemical Equations

To obtain the corresponding temporal changes of $[S_0]$, $[^3O_2]$, and $[^1O_2]_{rx}$, the information of light fluence rate (ϕ) distribution, and the measured Photofrin concentration are passed to the following time (t)-dependent

differential equations for a given treatment time point (10-13):

$$\frac{d[^3O_2]}{dt}+\left(\xi\frac{\phi[S_0]}{[^3O_2]+\beta}\right)[^3O_2]=g\left(1-\frac{[^3O_2]}{[^3O_2]_0}\right) \quad (1)$$

$$\frac{d[S_0]}{dt}+\left(\xi\sigma\frac{\phi([S_0]+\delta)[^3O_2]}{[^3O_2]+\beta}\right)[S_0]=0 \quad (2)$$

$$\frac{d[^1O_2]_{rx}}{dt}-\left(\xi\frac{\phi[S_0][^3O_2]}{[^3O_2]+\beta}\right)=0 \quad (3)$$

where, ξ, σ, β, δ, and g are the Photofrin photochemical parameters with definitions and values presented in Table 1. $[^3O_2]_0$ is the initial tissue oxygenation concentration, which is assumed to be 40 µM (14).

Table 1: Photofrin photochemical parameters (13)

Parameter	Definition	Value
ξ ($cm^2s^{-1}mW^{-1}$)	Specific oxygen consumption rate	3.7×10^{-3}
σ (μM^{-1})	Specific photobleaching ratio	7.6×10^{-5}
β (µM)	Oxygen quenching threshold concentration	11.9
δ (µM)	Low concentration correction	33
g (µM/s)	Maximum oxygen supply rate	0.76
$[^3O_2]_0$ (µM)	Initial ground-state oxygen concentration	40

4. Use of COMSOL Multiphysics® Software

The NDI acquired volume was imported into COMSOL Multiphysics (8,9). The delivered fluence values were also imported into COMSOL as 3D fluence clouds and were assigned to their respective positions (x, y, and z) on the NDI contour. Then, the forward calculation of the macroscopic kinetic equations (1)-(3) was performed in order to simulate $[^1O_2]_{rx}$ on the surface of the pleural cavity. Both homogeneous and heterogeneous distributions of the initial Photofrin uptake by the tissue was considered in the simulations. In the heterogeneous model, Photofrin uptake was considered to increase linearly in the z direction as $[S_0]$=0.047z- 0.011. Using this function, initial Photofrin concentration increases from 0.47 to 11.5 µM in the z direction.

5. Results

From 2004 to 2016, several patients aged from 27 to 81 years underwent surgical resection combined with PDT at the hospital of the University of Pennsylvania. Each patient received Photofrin (2 mg per kg body weight) with 24 hours before light exposure. Excitation light at 630 nm was delivered to a total fluence of 60 J/cm^2. For a representative mesotheioma patient, the light fluence, and $[^1O_2]_{rx}$ distributed on the surface of the plural cavity has been simulated.

5.1 Light fluence distribution on pleural cavity

The distribution of light fluence on the surface of the pleural cavity has been shown with a color map in Fig. 1. In the ongoing clinical trial, the prescribed light fluence dose for Photofrin-mediated PDT for mesothelioma is 60 J/cm^2. As shown in Fig. 1, the magnitude of the delivered fluence changes from 54.5 to 73.6 J/cm^2 on the surface of the pleural cavity.

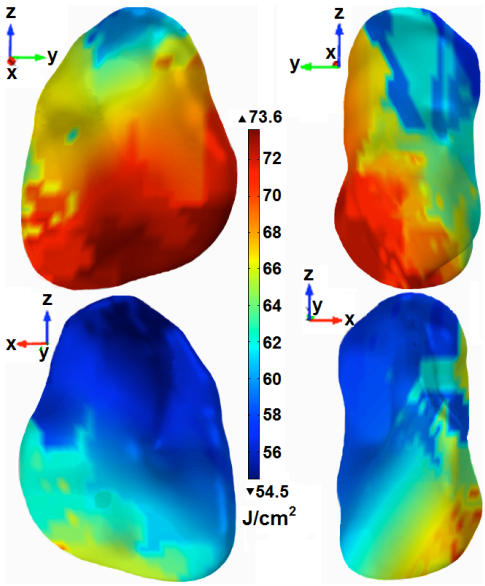

Figure 1. The light fluence distribution on the surface of the pleural cavity. The color bar shows the different magnitude of the fluence in J/cm^2.

5.2 Temporal changes of $[^3O_2]$ during PDT

As $^1O_2$ generation depends in part on the availability of $^3O_2$ in the target tissue, knowing the level of $[^3O_2]_0$, and $[^3O_2]$ during PDT is important (15,16). Tissue oxygenation is dependent on the metabolic requirements and functional status of each organ. However, to simplify the calculation, $[^3O_2]_0$ was considered to be 40 µM and homogeneously distributed in this model. Then, $[^3O_2]$ during PDT was calculated by using Eq. (1). Figure 2 shows the temporal changes of $[^3O_2]$ calculated for a particular ϕ and Photofrin concentration; ϕ = 75 mW/cm^2 and initial Photofrin concentration is 2.8 µM.

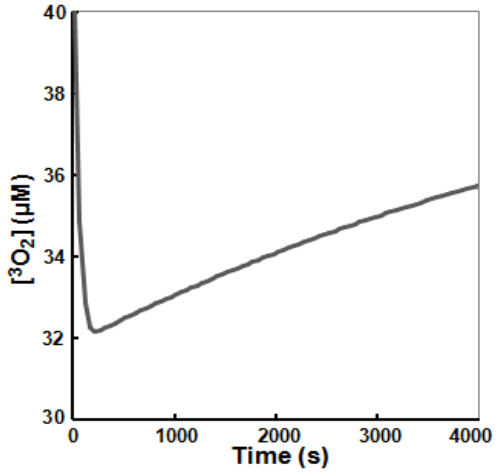

Figure 2. The consumption of the tissue oxygenation during Photofrin-mediated photodynamic therapy for $[^3O_2]_0$ = 40µM, ϕ = 75 mW/cm^2 and initial Photofrin concentration of 2.8 µM.

5.3 $[^1O_2]_{rx}$ calculated for a homogeneous Photofrin concentration on the surface of the pleural cavity

The generation of $^1O_2$ depends in part on the Photofrin concentration in the tumor tissue. Table 2 shows the results of the calculated $[^1O_2]_{rx}$ on the surface of the pleural cavity for ϕ = 75 mW/cm^2 and a homogeneous initial Photofrin concentration of 0.47, 2.8, 6.0, or 11.5 µM.

Table 2: $[^1O_2]_{rx}$ calculated for ϕ = 75 mW/cm^2 and homogeneous concentration of Photofrin

Photofrin (µM)	0.47	2.8	6.0	11.5
$[^1O_2]_{rx}$ (mM)	0.2	1.1	2.2	3.1

5.4 $[^1O_2]_{rx}$ calculated for a heterogeneous Photofrin concentration on the surface of the pleural cavity

The model presented in section 5.3 is very simplistic as in reality Photofrin uptake by tumor tissue is heterogeneous (6). In order to account for this heterogeneity, the initial Photofrin concentration was simulated to change from 0.47 to 11.5 µM in the z direction as shown in Fig. 3(a). Then, the corresponding $[^1O_2]_{rx}$ was calculated using ϕ = 75 mW/cm^2. Based on the results, $[^1O_2]_{rx}$ was calculated to be heterogeneous in the z direction. $[^1O_2]_{rx}$ increases from 0.2 to 4.5 mM in the z direction proportional to the increase in the Photofrin concentration (see Fig. 3(b)).

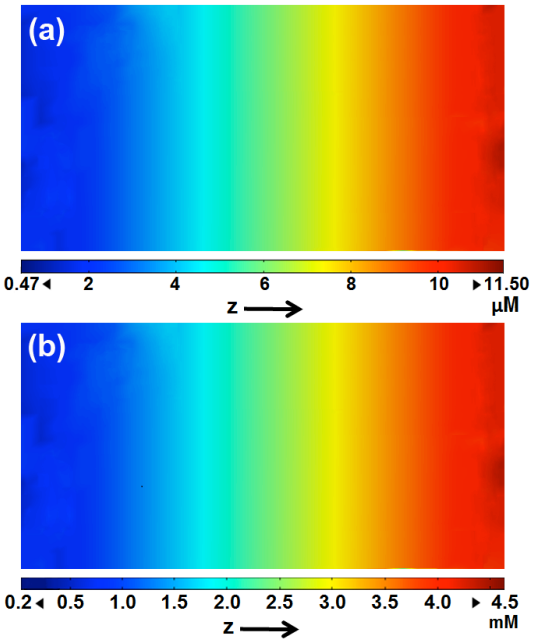

Figure 3. The heterogeneous distribution of (a) Photofrin concentration (at t = 0) in z direction, and (b) corresponding reactive singlet oxygen ($[^1O_2]_{rx}$) in the z axis. The calculations were done by using $[^3O_2]_0$ = 40 µM, and ϕ = 75 mW/cm^2. The color bars show the different magnitude of Photofrin in µM and $[^1O_2]_{rx}$ in mM.

Figure 4 presents the spatial distribution of $[^1O_2]_{rx}$ on the surface of the pleural cavity for a homogeneous initial tissue oxygenation of $[^3O_2]_0$ = 40µM, a constant light fluence rate of ϕ = 75 mW/cm^2 and heterogeneous drug distribution on the z axis.

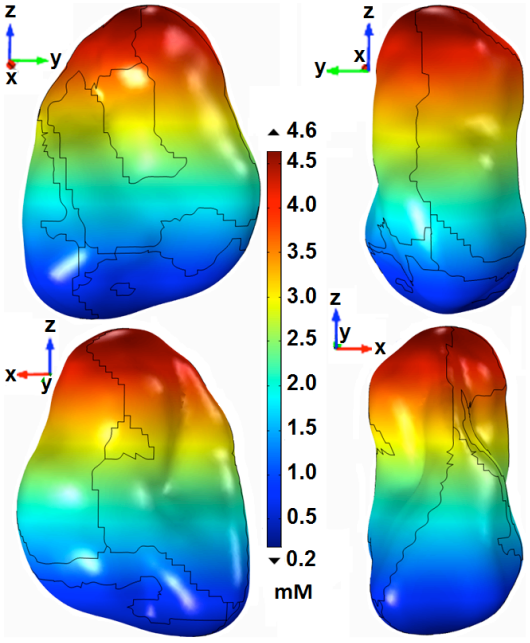

Figure 3. The distribution of $[^1O_2]_{rx}$ on the surface of the pleural cavity for $[^3O_2]_0 = 40$ µM, $\phi = 75$ mW/cm^2, and the heterogeneous distribution of 0.47-11.5 µM Photofrin in z direction. The color bar shows the different magnitude of $[^1O_2]_{rx}$ in mM.

6. Discussions

An ideal dosimetric predictor for PDT efficacy is still elusive due to the dynamic changes and interactions of the key PDT components, photosensitizer concentration, fluence (or light dose), and tissue $^3O_2$ level during treatment, which, to some extent, has hindered the clinical application of PDT. As the primary mediator of cell damage during type II PDT, $^1O_2$ has gained special attention as a good dosimetric quantity based on either direct measurements or indirect modeling (12,17). This study is focused on the latter method, due to the difficulty in directly measuring $[^1O_2]_{rx}$ in patients during PDT delivery.

In our calculations, tissue $[^3O_2]$ was considered to be homogeneous. Then, $[^1O_2]_{rx}$ was calculated for both homogeneous and heterogeneous Photofrin concentration in the tumor tissue. The spatial distribution of $[^1O_2]_{rx}$ on the surface of the pleural cavity was calculated to be 0.2, 1.1, 2.2 and 3.1 mM for 0.47, 2.8, 6.0 and 11.5 µM Photofrin, respectively. $[^1O_2]_{rx}$ showed an increase from 0.2 to 4.6 mM in the z direction proportional to the changes of the photosensitizer concentration from 0.47 to 11.5 µM in the same direction.

As published previously (18), when $[^1O_2]_{rx} \geq$ 1.1 mM, radiation-induced fibrosarcoma tumors exhibited a complete response to the Photofrin-mediated PDT. Based on the results of the current simulation, some regions are exposed to 1.1 mM $\geq [^1O_2]_{rx}$, and some regions are over-exposed to $[^1O_2]_{rx}$.

7. Conclusions

The distribution of $[^1O_2]_{rx}$ during PDT could be simulated and mapped on the treated plural cavity by using COMSOL Multiphysics.

The final target of this work will be to implement this method in real-time for clinical applications based on the measurements of the Photofrin concentration in different regions inside the pleural cavity. This helps us to account for the real photosensitizer heterogeneity instead of simulated one. We believe that *in situ* monitoring of the under- and over- exposed regions to $[^1O_2]_{rx}$ during treatment can significantly improve PDT for mesothelioma.

8. References

1. Penjweini, R., Loew, H.G., Breit, P., and Kratky, K.W., Optimizing the antitumor selectivity of PVP-Hypericin re A549 cancer cells and HLF normal cells through pulsed blue light. *Photodiagnosis and photodynamic therapy* **10**, 591-599 (2013)
2. Dougherty, T.J., Gomer, C.J., Henderson, B. W., Jori, G., Kessel, D., Korbelik, M., Moan, J., and Peng, Q., Photodynamic therapy. *J Natl Cancer Inst* **90**, 889-905 (1998)
3. Zhu, T.C., Kim, M.M., Jacques, S.L., Penjweini, R., Dimofte, A., Finlay, J.C., Simone, C.B., Cengel, K.A., and Friedberg, J., Real-time treatment light dose guidance of Pleural PDT: an update. *Proc. SPIE* **9308**, 930809 (2015)
4. Zhu, T.C., Liang, X., Kim, M.M., Finlay, J. C., Dimofte, A., Rodriguez, C., Simone, C. B., 2nd, Friedberg, J.S., and Cengel, K.A., An IR Navigation System for Pleural PDT. *Front Phys* **3** (2015)
5. Gallagher-Colombo, S.M., Quon, H., Malloy, K.M., Ahn, P.H., Cengel, K.A., Simone, C.B., 2nd, Chalian, A.A., O'Malley,

B.W., Weinstein, G.S., Zhu, T.C., Putt, M. E., Finlay, J.C., and Busch, T.M., Measuring the Physiologic Properties of Oral Lesions Receiving Fractionated Photodynamic Therapy. *Photochemistry and photobiology* **91**, 1210-1218 (2015)
6. Hahn, S.M., Putt, M.E., Metz, J., Shin, D. B., Rickter, E., Menon, C., Smith, D., Glatstein, E., Fraker, D.L., and Busch, T.M., Photofrin uptake in the tumor and normal tissues of patients receiving intraperitoneal photodynamic therapy. *Clinical cancer research : an official journal of the American Association for Cancer Research* **12**, 5464-5470 (2006)
7. Kim, M.M., Darafsheh, A., Ahmad, M., Finlay, J.C., and Zhu, T.C., PDT dose dosimeter for pleural photodynamic therapy. *Proc SPIE* **9694**, 96940Y (2016)
8. Penjweini, R., Kim, M.M., Dimofte, A., Finlay, J.C., and Zhu, T.C., Deformable medical image registration of pleural cavity for photodynamic therapy by using finite-element based method. *Proc SPIE* **9701**, 970106 (2016)
9. Penjweini, R., and Zhu, T.C., SU-E-J-111: Finite Element-Based Deformable Image Registration of Pleural Cavity for Photodynamic Therapy. *Medical Physics* **42**, 3290-3290 (2015)
10. Kim, M.M., Penjweini, R., and Zhu, T.C., In vivo outcome study of BPD-mediated PDT using a macroscopic singlet oxygen model. *Proc. SPIE* **9308**, 93080A (2015)
11. Penjweini, R., Kim, M.M., and Zhu, T.C., In-vivo outcome study of HPPH mediated PDT using singlet oxygen explicit dosimetry (SOED), *Proc. SPIE* **9308**, 93080N (2015).
12. Penjweini, R., Liu, B., Kim, M.M., and Zhu, T.C., Explicit dosimetry for 2-(1-hexyloxyethyl)-2-devinylpyropheophorbide-a-mediated photodynamic therapy: macroscopic singlet oxygen modeling. *Journal of biomedical optics* **20**, 128003 (2015)
13. Wang, K.K., Finlay, J.C., Busch, T.M., Hahn, S.M., and Zhu, T.C., Explicit dosimetry for photodynamic therapy: macroscopic singlet oxygen modeling. *J Biophotonics* **3**, 304-318 (2010)
14. Zhu, T.C., Liu, B., and Penjweini, R., Study of tissue oxygen supply rate in a macroscopic photodynamic therapy singlet oxygen model. *Journal of biomedical optics* **20**, 38001 (2015)
15. Penjweini, R., Kim, M.M., Finlay, J.C., and Zhu, T.C., Investigating the impact of oxygen concentration and blood flow variation on photodynamic therapy. *Proc SPIE* **9694**, 96940L (2016).
16. Penjweini, R., and Zhu, T. C., PDT study using a model incorporating initial oxygen concentration and blood flow increase. *Proc. COMSOL*, 1-5 (2015)
17. Niedre, M., Patterson, M.S., and Wilson, B.C., Direct near-infrared luminescence detection of singlet oxygen generated by photodynamic therapy in cells in vitro and tissues in vivo. *Photochemistry and photobiology* **75**, 382-391 (2002)
18. Qiu, H., Kim, M.M., Penjweini, R., and Zhu, T.C., Macroscopic singlet oxygen modeling for dosimetry of Photofrin-mediated photodynamic therapy: an in-vivo study. *Journal of biomedical optics* **21**, 88002 (2016)

9. Acknowledgements

This work is supported by grants from the National Institute of Health (NIH) R01 CA154562 and P01 CA87971.